Crystallographic Dependence of Chemisorption Bonding for Sulfur on (001), (110), and (111) Nickel

J. E. Demuth, D. W. Jepsen, and P. M. Marcus

IBM Thomas J. Watson Research Center, Yorktown Heights, New York 10598

(Received 25 February 1974)

The degree to which the surface atomic arrangement influences the bonding geometry of sulfur atoms on (001), (110), and (111) Ni surfaces is investigated by an analysis of experimental low-energy electron diffraction data. For all surfaces, the sulfur atoms reside in high-coordination sites—the atomic hollows of the surface; all nearest-neighbor Ni-S bond lengths are less than those of stable bulk compounds.

In several previous studies[1-6] the applicability of low-energy electron-diffraction (LEED) intensity-energy calculations to determine the structure of clean nickel surfaces and chemisorbed atoms on the (001) nickel surface has been demonstrated. Knowledge of the bond lengths and bond sites for crystallographically different surfaces is basic to an understanding of surface chemical bonding. Ion-neutralization spectroscopy[7] and LEED/radiotracer[8] studies have attempted to determine the geometric structure of chemisorbed sulfur overlayers on Ni(001), Ni(110), and Ni(111), but have obtained only qualitative information.

We report here a structural analysis for chemisorbed sulfur overlayers on (110) and (111) nickel surfaces which, together with our previous analysis on the (001) surface,[5-6] allows for the first time the crystallographic dependence of chemisorption bond sites and bond lengths to be examined. We also demonstrate that the LEED analysis which was successful for $c(2 \times 2)$ chalcogen structures on the (001) surface of nickel[4] is also applicable to $c(2 \times 2)$ and $p(2 \times 2)$ sulfur overlayers on the (110) and (111) surfaces of nickel, respectively. A general conclusion is that the Ni-S bond lengths found on all surfaces are smaller than those occurring in stable Ni-S bulk compounds, but are comparable to the bond length which occurs in the metastable γ phase of NiS (millerite).

The application of the layer-KKR (Korringa-Kohn-Rostoker) method to the calculation of LEED intensity-energy spectra is identical to that previously discussed.[2,4,5,9] Using the symmetries observed from the LEED pattern to fix the translational periodicity of the overlayer atoms, we then model the particular overlayer mesh on the surface for different registries with the substrate (bonding sites) and for a large number of vertical displacements $d_\perp$ from the sub-

strate. As previously described,[4,5] when the calculations are carried out over a sufficiently large energy range, the model geometry is the dominating factor in the theoretical spectra and the fit to experiment—in contrast to the effects of small variations in the atomic scattering potentials, in the degree of damping of the electrons, or in the Debye temperature of surface atoms. Hence, it is possible to make a clearcut discrimination between bonding geometries despite the uncertainties in the scattering potential and the surface boundary conditions, and despite the approximations in the theory (e.g., use of muffin-tin potentials and isotropic thermal motion).

In the model calculations, the self-consistent Hartree-Fock-Slater potential for Ni constructed by Wakoh[10] and a superposition potential for sulfur constructed by overlapping atomic charge densities were used. The S potential used for all calculations here was that found to describe best the experimental data from the (001) surface.[5,6] The Debye temperature in the adsorbed layer was set equal to that used for bulk nickel ($\theta_D = 420°K$), while electron damping in the overlayer was provided for by a 3-eV imaginary component in the potential. The inner potentials were obtained by adding the (small) measured change in work function[11] to the 11-eV inner potential determined previously[2] for the clean surface. For the $p(2 \times 2)$ structure the number of diffraction beams considered was doubled to 116 from the 58 beams used for the $c(2 \times 2)$ structures, since twice as many diffraction beams occur for this structure. As a consequence of this large number of beams necessary for the $p(2 \times 2)$ structure, the number of phase shifts used to describe the scattering from the atoms has been reduced to seven from eight.

The room-temperature experimental results for the sulfur structures on nickel that we ana-
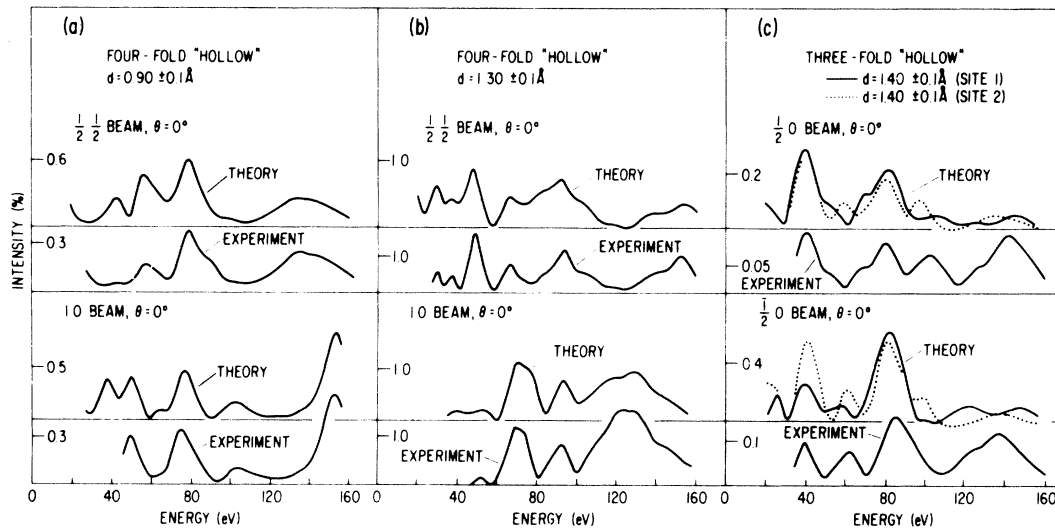
FIG. 1. Comparison of the calculated spectra with the experimental data of Demuth and Rhodin (Ref. 11) for (a) $c(2 \times 2)$, (b) $c(2 \times 2)$, and (c) $p(2 \times 2)$ sulfur overlayers on (110), (001), and (111) nickel, respectively.

lyze have been reported by Demuth and Rhodin.[11] The sulfur overlayer formed on (110) Ni had a translational periodicity characteristic of a $c(2 \times 2)$ structure similar to that formed in the (001) Ni surface. The translational periodicity for the sulfur overlayer on (111) Ni was characteristic of a $p(2 \times 2)$ structure. Interestingly, although the $c(2 \times 2)$ structure on (110) was formed by thermal diffusion of bulk sulfur contaminants to the surface in contrast to the method of decomposition of H_2S on the (001) and (111) surfaces, we determine surface geometries and bonding displacements similar to those found for the overlayers on the (001) and (111) surfaces. These two different methods of preparation also appear to give the same structure for $c(2 \times 2)$ sulfur overlayers on Ni(001).[6] Thus, it would appear that a nonreconstructed surface structure is favored by either of the experimental procedures used, as opposed to the forming of a bulk sulfide or a two-dimensional nickel sulfide phase.[8]

Representative comparisons showing the agreement achieved between theory and experiment for these sulfur structures on (110), (001), and (111) nickel surfaces are presented in Fig. 1 for several diffraction beams. Similar agreement has been achieved for the present-existing experimental data base which consists of the $\frac{1}{2}\frac{1}{2}$, 01, 10, 11, and 00 beam spectra on (110) and (001) surfaces and the $\frac{1}{2}0$ and $-\frac{1}{2}0$ and 00 beam spectra for the (111) surface. For the (110) and (001) surfaces we can easily select the bonding site

and displacement which best agree with experiment. For the (111) surface the comparison shows two threefold "hollow" sites for sulfur: The first has another threefold hollow site directly beneath it in the second nickel layer (site 1) and the second has a nickel atom directly beneath it in the second nickel layer (site 2). Although the distinction between these two threefold hollow sites in the calculated spectra is not as dramatic as was found for a $\sqrt{3} \times \sqrt{3}$ structure of I on Ag(111) by Forstman, Berndt, and Buttner,[12] the first threefold hollow site (site 1) is favored by the present experimental data base. This bonding position is similar to that found by Forstman, Berndt, and Buttner,[12] and also to that observed by Graham and Ehrlich[13] for W adatoms on W(111). For all surfaces the present small limitations in agreement between theory and experiment suggest further consideration of such factors as modifications in the adsorbate scattering potential due to differences in substrate crystallography as well as small distortions of surface atoms from their normal positions (in addition to the other factors previously mentioned). Additional considerations for the $p(2 \times 2)$ structure might include other small distortions of substrate atoms forbidden by symmetry in the $c(2 \times 2)$ structures.

The determined atomic locations for the sulfur atoms in these overlayer structures are illustrated in Fig. 2. The chemisorbed sulfur atoms reside in fourfold coordinated sites on the (110)
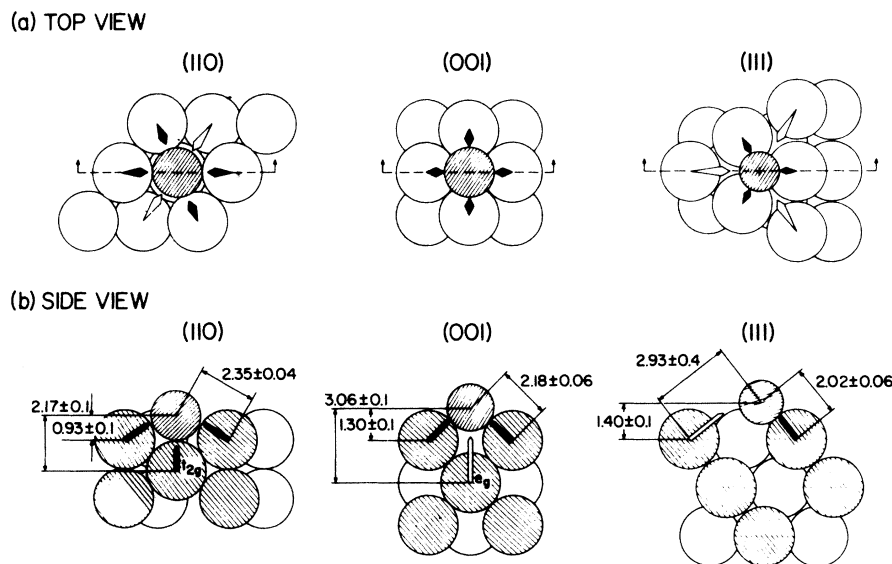
FIG. 2. Schematic diagram showing the determined atomic bonding sites of the sulfur atoms in the $c(2 \times 2)$, $c(2 \times 2)$, and $p(2 \times 2)$ structures on the (110), (001), and (111) nickel surfaces, respectively, as viewed from (a) above the surface (top view) or (b) from a cut-away section along the horizontal direction (side view). The preferred adsorption site on the (111) surface is the threefold hollow site which does not have another nickel atom below (site 1). The filled and open arrows represent e_g and t_{2g} molecular orbitals of the substrate, respectively.

and (001) surfaces and in the threefold coordinated site (site 1) on the (111) surface. These sites correspond to the positions which nickel atoms would occupy if an additional layer of nickel atoms were added. These sites also correspond to the directions in which d-electron molecular orbitals (e_g and t_{2g} symmetry) of the substrate point. These directions are indicated in Fig. 2 by the filled and open arrows, respectively. For the (110) surface, unlike the closer packed (001) and (111) surfaces, the sulfur atoms fit so deeply into the hollows that they are closer to the nickel atoms in the second substrate layer than to the nickel atoms in the first substrate layer. Note also that the sulfur atom lies closest to the surface plane of the (110) surface (as defined by the centers of the ion cores of the first atomic layer) and farthest from the surface plane of the (111) surface. However, the shortest Ni-S bond distance occurs on the (111) surface as compared to either the (001) or (110) surfaces (see Table I). This reduction of Ni-S bond length on the (111) surface can be associated with the reduction of the number of nearest-neighbor Ni atoms to the adsorbed sulfur atom, thereby increasing the bond energy and reducing the Ni-S bond length relative to the (001) or (110) surfaces.[14]

For all surfaces our determined Ni-S bond lengths are smaller than stable bulk-compound lengths of 2.28, 2.34, and 2.38 Å for Ni_3S_2, NiS_2, and α-NiS, respectively.[4,5] However, a metastable γ-NiS bulk phase known as millerite[15] exists which is structurally similar to our determined sulfur structures on Ni(001) and Ni(110). This γ phase of NiS occurs in nature and has a nearest-neighbor Ni-S bond length of ~ 2.18 Å with sulfur atoms nearest four nickel neighbors.

The authors would like to express their appreciation to Professor T. N. Rhodin for use of ex-

TABLE I. Summary of bond distances (in Å) where $d_\perp$ is the displacement of the center of the adsorbed sulfur atom from the surface plane of Ni and d_m and d_{mn} refer to nearest- and next-nearest-neighbor Ni-S bond distances. The number of nearest and next-nearest Ni neighbors per sulfur atom is given in parentheses. Interlayer spacings for the clean (110), (001), and (111) Ni surfaces are 1.24, 1.76, and 2.03 Å, respectively.

Ni-S	(110)	(001)	(111)
$d_\perp$	0.93 ±0.1	1.30 ±0.1	1.40 ±0.1
d_m	2.17 ±0.1 (1)	2.18 ±0.06 (4)	2.02 ±0.06 (3)
d_{mn}	2.35 ±0.04 (4)	3.06 ±0.1 (1)	2.93 ±0.04 (3)

perimental data prior to publication and to Professor F. Jelinek for several helpful comments regarding bulk Ni-S compounds.

[1]S. Andersson and J. B. Pendry, J. Phys. C: Proc. Phys. Soc., London 5, 41 (1972).

[2]J. E. Demuth, P. M. Marcus, and D. W. Jepsen, in Proceedings of the Seventh Low-Energy Electron Diffraction Symposium, San Diego, California, March 1973 (to be published).

[3]G. E. Laramore, Phys. Rev. B 8, 515 (1973).

[4]J. E. Demuth, D. W. Jepsen, and P. M. Marcus, Phys. Rev. Lett. 31, 540 (1973).

[5]J. E. Demuth, D. W. Jepsen, and P. M. Marcus, Solid State Commun. 13, 1311 (1973).

[6]J. E. Demuth, D. W. Jepsen, and P. M. Marcus, to be published.

[7]H. D. Hagstrum and G. E. Becker, Surface Sci. 30, 505 (1972).

[8]M. Perdereau and J. Oudar, Surface Sci. 20, 80 (1970).

[9]D. W. Jepsen, P. M. Marcus, and F. Jona, Phys. Rev. B 6, 3864 (1972).

[10]S. Wakoh, J. Phys. Soc. Jap. 20, 1984 (1965).

[11]J. E. Demuth and T. N. Rhodin, to be published.

[12]F. Forstman, W. Berndt, and P. Buttner, Phys. Rev. Lett. 30, 17 (1973).

[13]W. R. Graham and G. Ehrlich, J. Chem. Phys. 59, 3417 (1973).

[14]L. Pauling, The Nature of the Chemical Bond (Cornell Univ. Press, New York, 1964).

[15]S. G. Gmelin, Handbuch der Anorganischen Chemie (Verlag Chemie, Weinheim/Bergstrasse, Germany, 1966), Vol. 57, Part 2, p. 657.

Direct Evidence of Pretransformation Lattice Instabilities

H. C. Tong and C. M. Wayman

Department of Metallurgy and Mining Engineering and Materials Research Laboratory, University of Illinois at Urbana-Champaign, Urbana, Illinois 61801

(Received 11 March 1974)

Observations on lattice instability are demonstrated by transmission and diffraction electron microscopy together with an electron multiplier. The latter displays the coupled atomic fluctuations on an oscilloscope screen. The WKB method has been used to calculate a single-atom transition time. The results indicate that fluctuations should be present and that quantum mechanical considerations are important in the nucleation of solid-state phase transformation. A standing-wave model is suggested for the pretransition lattice instabilities and is experimentally supported.

A number of alloys undergoing phase transitions apparently exhibit soft phonon modes when cooled to a temperature approaching the critical temperature for the structural transition. Of recent interest have been the alloys V_3Si and Nb_3Sn.[1] At high temperatures, these materials possess the β-tungsten structure, but at lower temperatures they undergo a cubic-to-tetragonal martensitic transition. These alloys are reported to exhibit the superconducting state a few degrees below the martensite start temperatures ($M_s = 22$ and $43°K$, respectively, for V_3Si and Nb_3Sn). In addition, the elastic anisotropy factor $A = 2C_{44}/(C_{11} - C_{12})$ is large for these materials near the transition temperature, which indirectly indicates a lattice softening behavior. The observed lattice instability has been viewed as a band Jahn-Teller effect.[2] However, it should be noted that Au-Cd,[3] Au-Cu-Zn,[4] and In-Tl alloys[5] also undergo martensitic transformations and show a large elastic anisotropy near the M_s temperature. It has been noted especially that $C_{11} - C_{12} \to 0$ as $T \to M_s$ for β-Au-Cu-Zn alloys.[4] Since not all of these alloys are based on transition elements and none exhibits the β-tungsten structure, the universal importance of the Jahn-Teller interpretation can be questioned. However, certain common characteristics apply to the previous alloys: All undergo structural phase transitions without compositional change, and as the transformation proceeds, the product phase is "connected" to the parent in a highly coherent manner, typical of thermoelastic martensitic transformations. Since Cu-Zn,[6] Ag-Cd,[7] Ni-Ti,[8] Fe-Pt,[9] Cu-Au,[10] Fe-Ni,[11] and other alloys have the same common characteristics, lattice instabilities in these cases might also be expected.

The direct observation of lattice instabilities can be made by studying the in situ transformation process and kinetics with a controllable heat-